Phospholipase A_2 Engineering. Deletion of the C-Terminus Segment Changes Substrate Specificity and Uncouples Calcium and Substrate Binding at the Zwitterionic Interface[†,▽]

Baohua Huang,[‡,§] Bao-Zhu Yu,[∥] Joseph Rogers,[∥] In-Ja L. Byeon,[⊥] Kanagaraj Sekar,[⊥] Xin Chen,[#] Muttaiya Sundaralingam,*[,‡,⊥,#] Ming-Daw Tsai,*[,‡,⊥,#] and Mahendra K. Jain*[,∥]

Departments of Chemistry and Biochemistry and The Ohio State Biochemistry Program, The Ohio State University, Columbus, Ohio 43210, and Department of Chemistry and Biochemistry, University of Delaware, Newark, Delaware 19716

Received January 30, 1996; Revised Manuscript Received May 8, 1996[⊗]

ABSTRACT: It has been suggested [Dijkstra, B. W., Drenth, J., & Kalk, K. H. (1981) *Nature 289*, 604−606] that the interfacial binding site of phospholipase A_2 (PLA2) involves a large number of residues, including a cluster at the N-terminus and another cluster at the C-terminus. The approaches of multiple mutation and deletion were used to test the roles of the C-terminal residues of bovine pancreatic PLA2 overexpressed in *Escherichia coli*. A double mutant K120A/K121A and a deletion mutant Δ115−123/C27A were constructed, and structural and functional analyses were performed on both mutants. The double mutant showed little perturbation in the global structure on the basis of proton NMR and X-ray crystallographic analyses. The proton NMR analysis of the deletion mutant suggested that a few residues at the active site, the hydrophobic channel, and the calcium binding loop are perturbed, but the global conformation is not changed. The mutants were then characterized for catalytic and binding properties by use of various kinetic and spectroscopic methods. The double mutant behaved in a manner similar to that of the wild type (WT) PLA2 in every property examined. The deletion mutant was found to show an interesting change of substrate specificity. The $k_{cat,app}$ of the zwitterionic DC_8PC micelles but not the anionic DC_8PM micelles decreased by a factor of >100; however, the activity of DC_8PC was restored upon addition of 4 M NaCl. The results of fluorescence spectroscopic studies indicate that the deletion mutant behaves in a manner similar to that of WT in the binding to anionic vesicles and to zwitterionic neutral diluent. Thus, the binding affinity of the enzyme to the interface (the E to E* step) should not be the main cause for the change in substrate specificity. The cause lies at least partially in the binding of substrate or inhibitor to the active site of the enzyme at the interface, i.e., the E* to E*L step, as revealed by the results of equilibrium binding studies. The equilibrium dissociation constants of ligands are generally higher for the deletion mutant (relative to WT) at the zwitterionic interface but not at the anionic interface. The cause for the low affinity of an active site-directed ligand to the active site at the zwitterionic interface could be related to the inability of Ca^{2+} to enhance ligand binding for the deletion mutant. This is in contrast to the WT PLA2 for which Ca^{2+} binding enhances binding of the substrate to the active site. Overall, the structural and functional perturbations caused by deleting the C-terminal segment are modest, but the changes in substrate specificity and the uncoupling between substrate and calcium binding are interesting and significant.

One of the important structural elements for the catalytic reaction of phospholipase A_2 (PLA2)[1] is the interfacial recognition (binding) site (Dijkstra et al., 1981, 1984; Scott et al., 1990; Ramirez & Jain, 1991). The interfacial binding site is a unique feature of PLA2 since it has been established that the binding of PLA2 to the substrate interface must precede the catalytic turnover at the interface (Jain et al., 1986) and that binding of the enzyme to the interface increases its affinity for the active site-directed ligands (Jain et al., 1993). On the basis of the crystal structure of bovine pancreatic PLA2, Dijkstra et al. (1981) proposed that the interfacial binding face, as shown in Figure 1, involves a

[†] This work was supported by Research Grants GM41788 (to M.-D.T.), GM29703 (to M.K.J.), and GM49547 (to M.S.) from the National Institutes of Health. The Bruker AM-500 NMR spectrometer used was funded by NIH Grant RR01458.

[▽] This is paper 16 in the series Phospholipase A_2 Engineering. For paper 15, see Zhu et al. (1995). It is also paper 5 in the series Crystallography of Phospholipase A_2; for paper 4, see Liu et al. (1995).

[‡] The Ohio State Biochemistry Program, The Ohio State University.

[§] Current address: Department 47G, Abbott Laboratories, Abbott Park, IL 60064.

[∥] University of Delaware.

[⊥] Department of Chemistry, The Ohio State University.

[#] Department of Biochemistry, The Ohio State University.

[⊗] Abstract published in *Advance ACS Abstracts,* September 1, 1996.

[1] Abbreviations: BSA, bovine serum albumin; CD, circular dichroism; COSY, correlated spectroscopy; 1D, one-dimensional; 2D, two-dimensional; DC_8PC, 1,2-dioctanoyl-*sn*-glycero-3-phosphocholine; DC_8PM, 1,2-dioctanoyl-*sn*-glycero-3-phosphomethanol; $DC_{14}PM$, 1,2-dimyristoyl-*sn*-glycero-3-phosphomethanol; DTPM, 1,2-ditetradecyl-*sn*-glycero-3-phosphomethanol; EDTA, ethylenediaminetetraacetate; EGTA, ethylene glycol bis(β-aminoethyl ether)-*N*,*N*,*N*′,*N*′-tetraacetic acid; FPLC, fast protein liquid chromatography; GB, Gaussian broadening; GdnHCl, guanidine hydrochloride; LB, line broadening; MJ33, 1-hexadecyl-3-(trifluoroethyl)-*rac*-glycero-2-phosphomethanol; NOE, nuclear Overhauser effect; NOESY, nuclear Overhauser enhancement spectroscopy; pH*, pH in D_2O without correcting for the deuterium isotope effect; PLA2, phospholipase A_2; pyrene-PM, 1-hexadecanoyl-2-(1-pyrenyldecanoyl)-*sn*-glycero-3-phosphomethanol; TMSP, sodium 3-(trimethylsilyl)[2,2,3,3-d_4]propionate; WT, wild type.

S0006-2960(96)00234-6 CCC: $12.00

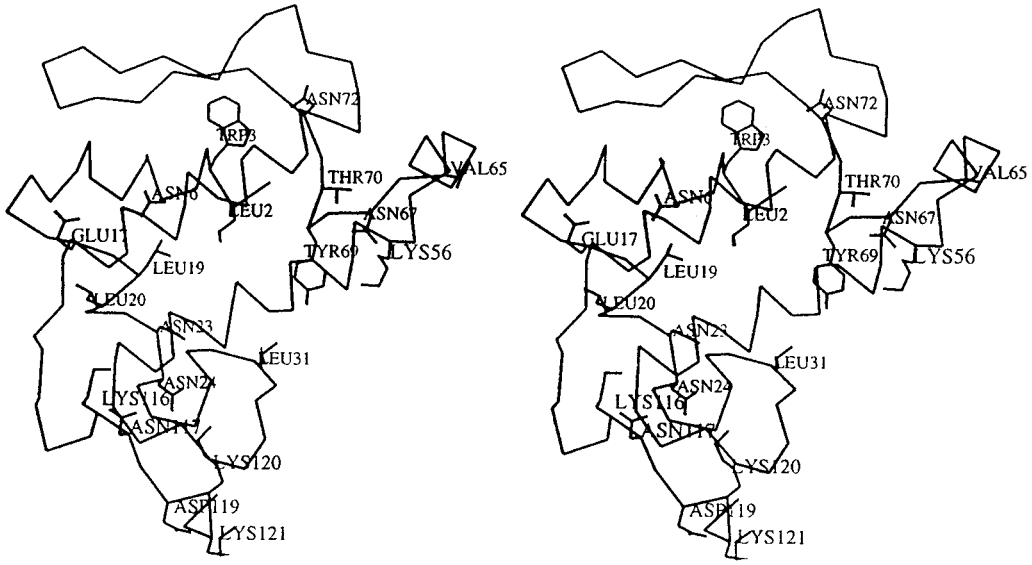

FIGURE 1: Interfacial binding site proposed by Dijkstra et al. (1981, 1984). Reconstructed from the bovine pancreatic PLA2 crystal structure (Noel et al., 1991).

cluster of N-terminal residues (Ala-1, Leu-2, Trp-3, and Asn-6), a cluster of C-terminal residues (Lys-116, Asn-117, Asp-119, Lys-121, and Lys-122), and several other residues.

The roles of these interfacial binding residues have been investigated extensively earlier by chemical modification and spectroscopic studies (Ramirez & Jain, 1991, and references therein). In an effort to further refine the interfacial binding site and understand the importance of these residues in interfacial catalysis, we have used site-directed mutagenesis in conjunction with structural and functional analyses to investigate possible interfacial site residues Lys-56 (Noel et al., 1990, 1991) and the N-terminal residues (Maliwal et al., 1994; Liu et al., 1995). Site-directed mutagenesis has also been used to probe the roles of Leu-31 (Kuipers et al., 1990).

We have now turned our attention to the C-terminus residues and have approached the problem with multiple mutation and deletion on the basis of two considerations. Firstly, the results from previous studies indicated that the effects of mutations of individual residues in the interfacial binding site are usually small and incremental; changing more than one residue is more likely to produce noticeable effects. Secondly, although PLA2 from bovine pancreas is tightly packed in a rigid, globular form, the last nine residues of the C-terminus seem to be structurally dispensable. These residues are loosely packed with little secondary structure except that the last residue (Cys-123) is linked to the main structure *via* a disulfide bond with Cys-27. This disulfide bond is absolutely conserved among the 46 natural variants of PLA2 whose sequences have been aligned by Heinrikson (1991). Thus, it is interesting to test the effects of deleting the entire C-terminal segment on the structure, interfacial binding, and catalysis. The results of this work suggest that the overall structural and functional roles of the C-terminal residues are modest, but the C-terminus deletion mutant displays an interesting and significant property. It functions well at the anionic interface, but its activity decreases substantially at the zwitterionic interface possibly due to the uncoupling between calcium binding and substrate (inhibitor) binding.

MATERIALS AND METHODS

Materials. Oligonucleotide primers were purchased from Midland Certified Reagent Co. (Midland, TX). Oligonucleotide-directed Mutagenesis kit (Version 2.11) and Sequencing kit Version 2.0 were purchased from Amersham and United States Biochemical, respectively. All restriction enzymes and incubation buffers were obtained from Boheringer. Reduced glutathione and oxidized glutathione were purchased from Calchem. T4 polynucleotide kinase was from NEB. IPTG was from Research Organics. The lipid substrate DC_8PC for the PLA2 assay was purchased from Avanti Polar Lipids (Alabaster, AL). The following lipids were synthesized as described previously: DTPM (Jain et al., 1986), $DC_{14}PM$ (Jain & Gelb, 1991), and MJ33 (Jain et al., 1991c). Ultrapure guanidine hydrochloride was purchased from ICN Biochemicals. The 99.9% D and 99.96% D D_2O were purchased from ISOTEC (Miamisburg, OH) and CIL, respectively. TMSP was obtained from MSD Isotopes. DCl and NaOD were purchased from Cambridge Isotopes.

Routine Procedures. Dideoxy sequencing of single-stranded DNA of M13 origin using [α-^{35}S]ATP was performed according to the protocol supplied with the Sequenase kit using the kit from United States Biochemical. This protocol for isolation of single-stranded M13 DNA is from the manual of the "oligonucleotide-directed *in vitro* mutagenesis system" available from Amersham. Routine DNA miniprep for isolation of plasmid DNA was performed according to the alkaline miniprep protocol described in *Molecular Cloning*.

Construction of Mutants. Site-directed mutagenesis was performed according to protocol from the manual of the "oligonucleotide-directed *in vitro* mutagenesis system" available from Amersham. The mature PLA2 gene from the pTO-A2M plasmid (Deng et al., 1990) was used to construct the mutants. The double mutant K120A/K121A was constructed from oligonucleotide 5′CCA AGC TTA ACA GTT AGC AGC ATC AAG ATT CTT GTG3′. The deletion mutant Δ115−123/C27A was constructed from oligonucleotides 5′CC ACA ATA AGC ACC ATA ATT3′ (C27A) and 5′CCG GAT CCA AGC TTA TTC TTT GTT ATA AGG TAC3′ (Δ115−123). The resulting mutants were verified by sequencing the single-stranded phage DNA by use of the dideoxy-chain-termination method (Sanger et al., 1977).

Purification of Mutants. Recombinant PLA2 and mutants were isolated from *Escherichia coli* strain BL21(DE3)-

[pLysS] carrying the pTO plasmid with the PLA2 gene as described elsewhere (Noel et al., 1991; Dupureur et al., 1992a,b; Li & Tsai, 1993). The routine large scale preparation of PLA2 was achieved by the growth of 10 L of culture in rich medium.

NMR Analysis. NMR experiments were performed on a Bruker AM-500 spectrometer at 37 °C. The sample preparation was as follows. PLA2 (ca. 10 mg) was dissolved in 0.5 mL of D_2O (99.9 at. % D) containing 300 mM NaCl and 50 mM $CaCl_2$. The sample was kept at room temperature for 4 h to allow for deuterium exchange, followed by lyophilization. After the exchange step was repeated, the sample was dissolved in 0.5 mL of "100%" D_2O and the pH* (uncorrected pH directly from pH meter reading) was adjusted to 4.0 by using DCl and NaOD stock solutions. TMSP was used as an internal chemical shift reference. Solvent suppression by presaturation was applied in all experiments.

GdnHCl-Induced Denaturation and Conformational Stability. CD spectra were recorded on a JASCO J-500C spectropolarimeter using a thermostated quartz microcell and processed using DP-500/AT system (version 1.29) software. A stock solution of ca. 8.5 M GdnHCl was prepared in a buffer containing 10 mM borate and 0.1 mM EDTA at pH 8.0, and the exact concentration was determined by refractive index (Nozaki, 1972). An enzyme solution of approximately 3 mg/mL was prepared in the same buffer, and the precise concentration was measured spectrophotometrically. Samples, which contained 0.05 mg/mL enzyme, the borate buffer mentioned above, and various concentrations of GdnHCl, were incubated at 30 °C for 10 min and then scanned five times from 250 to 200 nm. The ellipticity at 222 nm was recorded and used to determine the free energy of unfolding $\Delta G_d^{H_2O}$ according to the equation below (Pace, 1986):

$$\Delta G_d = \Delta G_d^{H_2O} - m[\text{GdnHCl}]$$

where ΔG_d is the Gibbs free energy of denaturation at various GdnHCl concentrations, $\Delta G_d^{H_2O}$ is the Gibbs free energy extrapolated to zero GdnHCl concentration, and m is a constant related to the susceptibility of the enzyme to the denaturation by the denaturant. A plot of ΔG_d versus [GdnHCl] at the transition region of the denaturatiuon curve gives $\Delta G_d^{H_2O}$, the free energy of unfolding at zero GdnHCl concentration as the intercept.

X-ray Crystallography of K120A/K121A. Crystals were grown by the hanging drop vapor diffusion method using the conditions described for the WT enzyme (Noel et al., 1991). The crystals belong to the trigonal system with space group $P3_121$ and cell parameters $a = b = 46.81$ Å and $c = 102.89$ Å. A crystal of size 0.4 × 0.3 × 0.4 mm was used for data collection. The intensity data were collected on our in-house *R*-axis II image plate to a resolution of 1.9 Å. The X-ray generator was powered at 50 kV and 100 mA. Unique reflections (10 032) were measured with an R_{sym} of 7.5%. The coordinates of the WT PLA2 (Noel et al., 1991) were used as the starting model for refinement because this mutant crystal was isomorphous. The structure was refined using X-PLOR 3.0 (Brunger, 1992). After several cycles of positional and simulated annealing refinements, difference electron density maps were calculated and used to fit the protein model by using the molecular-modeling program FRODO (Jones, 1985). Only minor rebuilding was needed. Water molecules were located from the difference electron density maps with heights greater than 3σ and at hydrogen-bonding distances of 3.6 Å or less to protein polar atoms or other water molecules. Refinement of the structure including water molecules gave a final R value of 19.2% for the 8755 reflections with $F > 2\sigma(F)$ in the 8.0−1.9 Å resolution range. All atoms were refined with unit occupancies. The final model consists of 949 protein atoms, 1 calcium ion, and 81 water molecules.

Protection Studies for the Determination of Interfacial Dissociation Constants. A protocol based on the relative rates of alkylation of the catalytic residue His-48 of PLA2 was used to monitor interfacial equilibria for the ligands bound to the active site of the enzyme at the interface (Jain et al., l991a). Assay of residual activity in the protection assay was carried out as described before (Yu et al., 1993). As is the case with the wild type enzyme, for most mutants, alkylation by *p*-nitrophenacyl bromide was reasonably rapid. For these measurements, typically, 0.1−1 μM PLA2 was incubated at 22 °C in a 6 × 50 mm borosilicate glass tube with 0.03 mL of reaction mixture containing 50 mM cacodylate buffer, 0.1 M NaCl, 0.03 mg of γ-globulin, and 2 mM *p*-nitrophenacyl bromide at pH 7.3 in the presence or absence of 1.65 mM deoxy-LPC, in 0.5 mM Ca^{2+} or 13 mM EGTA and other appropriate ligands. At various time intervals, an aliquot of the above reaction mixture containing 0.01−10 pmol of the enzyme was added to 1.5 mL of fluorescent lipid assay solution containing 1 μg of pyrene-PM (Molecular Probes), 250 μg of BSA (Sigma), 0.1 M NaCl, 0.25 mM $CaC1_2$, and 50 mM Tris buffer at pH 8.5 and 22 °C. The fluorescent lipid assay was pre-equilibrated for 2−3 min before addition of the reaction mixture for alkylation, until a stable baseline was obtained. The residual activity was detected as a function of time on a SLM 4800S spectrofluorimeter at an excitation wavelength of 345 nm and an emission wavelength of 395 nm with a 4 nm slit width for both excitation and emission.

Some changes in the conditions were necessary for the mutants. For the double mutant K120A/K121A, the incubation was carried out at 5 mM deoxy-LPC and 0.03 mM enzyme because its apparent affinity for the zwitterionic interface was somewhat lower. For the Δ115−123/C27A deletion mutant, higher concentrations of Ca^{2+} (3 mM) and enzyme (0.05 mM) were necessary for the incubation because of high K_{Ca} values and low turnover rates. The kinetic properties of the deletion mutant are appreciably affected by the presence of salt in the reaction mixture; therefore, the equilibrium constants were also measured in the presence of 4 M NaCl. The half-time for the alkylation of the deletion mutant was considerably longer with *p*-nitrophenacyl bromide, and therefore, phenacyl bromide (Aldrich, recrystallized from hexane) was used as the alkylating agent. Since the activity of the deletion mutant is very low ($^1/_{5000}$ compared to that of WT) in the fluorescence assay under the conditions described above, 4 M NaCl was used in the assay mixtures; the observed rate is higher by a factor of 60.

Kinetic Analysis. Initial rate measurements for the hydrolysis of phospholipid dispersions were carried out by pH-stat titration with a Brinkmann (Metrohm) titrimeter at room temperature. Substrate was equilibrated at pH 8.0 in 4 mL of water with the appropriate concentration of salt and 10 mM $CaCl_2$ for zwitterionic lipids, but with only 1 mM $CaC1_2$ for anionic lipids, at pH 8.0 under a stream of nitrogen (Jain et al., 1986a). Polymyxin B (20 μg) was added to the

reaction mixture containing $DC_{14}PM$ vesicles. Under these conditions, the initial rate of hydrolysis, v_o, at the maximum mole fraction of the substrate, $X_s = 1$, can be obtained for several minutes. Polymyxin B promotes substrate replenishment (Jain et al., 1991b), which is not necessary with DC_8-PM micelles where the spontaneous exchange of phospholipids is rapid. Also, it has been shown that polymyxin B promotes direct vesicle−vesicle exchange of monoanionic phospholipids through intervesicle contacts (Cajal et al., 1996). Under the conditions employed for kinetic measurements with anionic vesicles, polymyxin B promotes formation of clusters of several vesicles and phospholipid molecules in the outer monolayer of these vesicles exchange rapidly through these contacts. Thus, the substrate replenishment under the kinetic conditions is rapid, and the chemical step remains rate-limiting (Jain et al., 1992).

The reaction was started by addition of enzyme, and steady state rates were measured for at least 3 min. If inhibitor or other components were present in the reaction mixture, they were added before the reaction was initiated with enzyme. Controls showed that the order of addition did not significantly affect the appearance of the reaction progress curve. The amount of enzyme (0.5−20 pmol) used varied with substrate, amount of substrate, mutant, and salt condition. Typically, less enzyme was needed for the hydrolysis of short-chain phosphatidylcholines at 4 M NaCl than at 0.1 M NaCl. The initial rates for DC_8PC have uncertainty less than 10%. $K_{m,app}$ and $k_{cat,app}$ were calculated from nonlinear regression fit to a rectangular hyperbola, and standard deviations were less than ±15%.

Scooting mode kinetic analyses using $DC_{14}PM$ vesicles were conducted as described previously under first-order (Jain et al., 1986; Jain & Gelb, 1991; Berg et al., 1991) or zero-order (Berg et al., 1991; Jain et al., l991b) conditions. The turnover number at the maximal mole fraction of the substrate (v_o),[2] the apparent second-order rate constant ($N_S k_i$), and the interfacial Michaelis constant (K_M*) were obtained by deconvolution of the reaction progress curve and by equations involving various combinations of equilibrium and kinetic parameters (Jain et al., 1995).

The value of K_M* was calculated by three independent methods: (a) from the integrated Michaelis−Menten equation to describe the whole reaction progress curve (Berg et al., 1991); (b) from a relationship between K_I* and the mole fraction of the inhibitor required for 50% inhibition, $X_I(50)$ (Jain et al., 1991a); and (c) from K_{Ca}* and K_{Ca}*(S), the apparent dependence of v_o on the calcium concentration (Yu et al., 1993). The uncertainty in these values is about ±15% on the basis of standard deviations.

Spectroscopic Methods. As described previously (Dupureur et al., 1992a; Jain et al., 1993), all spectroscopic measurements were made in 10 mM Tris·HCl buffer at pH 8.0 and 22 °C. The steady state fluorescence measurements were carried out on a SLM-Aminco AB2 spectrophotometer at an excitation wavelength of 292 nm and emission at 333 nm for Trp-3 or at 490 nm for the resonance energy transfer measurement to the dansyl lipid acceptor. The slit width was 4 nm for both excitation and emission. Binding of PLA2 to DTPM vesicles was studied by monitoring the change of the fluorescence emission of the tryptophan residue (Trp-3) on PLA2 with the addition of DTPM. The Tris solution contains 3 μM protein, 0.1 mM $CaC1_2$, and NaCl at indicated concentrations.

Binding of ligands to the enzyme at the interface of deoxy-LPC as the neutral diluent was measured by monitoring the change of UV absorption spectra in the 250−350 nm range on a Hewlett-Packard 8452 spectrophotometer equipped with a diode array detector. The difference spectra and correction of turbidity were carried out with the software package provided with the instrument. Typically, titration with the active site-directed ligands was carried out in 10 mM Tris buffer containing 3 mM deoxy-LPC, 40 μM protein, and the appropriate amount of $CaCl_2$ and NaCl.

RESULTS

Construction and Purification of Mutants. Two mutants were used in this study. The double mutant K120A/K121A was constructed to test the roles of the positively charged side chains of these two lysine residues. The deletion mutant Δ115−123/C27A was used to test the deletion of the entire C-terminal segment. Since Cys-123 forms a disulfide bond with Cys-27 in the wild type PLA2, Cys-27 was also changed to Ala to avoid a free cysteine that may form incorrect disulfide bonds with other cysteines (Zhu et al., 1995). The construction of mutants, refolding, and purification are described in Materials and Methods.

Proton NMR. The 1D proton NMR spectra of WT, K120A/K121A, and the deletion mutant are shown in Figure 2. The spectrum of K120A/K121A is very similar to that of WT, and that of the deletion mutant is moderately perturbed. As a way to quantitatively evaluate the changes between WT and the mutants, 2D NOESY spectra were obtained as shown in Figure 3. Some of the resonances were assigned and are listed in Table 1. The resonance assignment for WT PLA2 was obtained from the previous work (Dupureur et al., 1992a,b; Fisher et al., 1989), which was based mainly on 2D NOESY and COSY experiments and used the crystal structure as a reference. Although the total assignment and structural determination of *porcine* pancreatic PLA2 by NMR have been completed (van den Berg et al., 1995), those of *bovine* pancreatic PLA2 used in our work are still in progress in our lab. The resonance assignments for the mutants were based on direct comparison of the 1D and NOESY spectra those of with WT PLA2.

As shown in Table 1, the assigned chemical shifts of the double mutant are very similar to those of WT PLA2, indicating that the conformation of the double mutant is virtually unperturbed from that of WT PLA2. On the other hand, there are notable changes in the deletion mutant. Several spin systems (F5, Y111, Y69, F22, Y28, I9, and L41) that have been assigned for WT (Dupureur et al., 1992a,b) could not be readily assigned for the deletion mutant. However, those assigned are strikingly similar (within 0.1 ppm) to the corresponding resonances of WT. A possible

[2] Definition of kinetic parameters *at the interface*: K_{Ca}*, dissociation constant for Ca^{2+} determined by the protection method; K_{Ca}*(S), effective dissociation constant for Ca^{2+} under catalytic conditions at a mole fraction of 1 of the substrate; K_I*, dissociation constant of inhibitor; K_M*, interfacial Michaelis constant; K_{ND}, apparent dissociation constant for the binding of the neutral diluent to the active site of the enzyme at the interface; K_P*, dissociation constant of product; K_S*, dissociation constant of substrate; k_{cat}, turnover number at saturating substrate concentration; $N_S k_i$, apparent second-order rate constant (apparent rate constant for the hydrolysis in the scooting mode under the substrate-limiting condition); v_o, turnover number at $X_S = 1$; X_I, mole fraction of inhibitor; $X_I(50)$, mole fraction of the inhibitor required for 50% inhibition. It should be noted that notations K_I*, K_M*, K_P*, and K_S* correspond to the conventional K_I, K_M, K_P, and K_S, respectively, used previously (Berg et al., 1991).

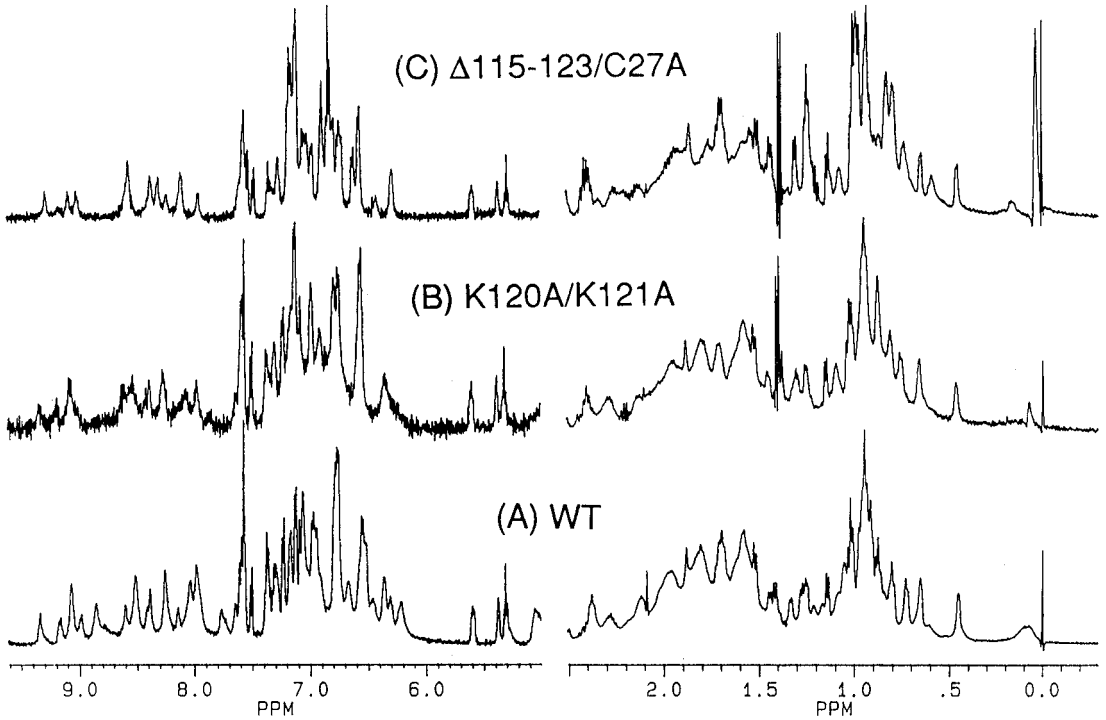

FIGURE 2: One-dimensional proton NMR spectra of WT and the three mutants in D_2O at 500 MHz. Sample conditions were as follows: 1.5 mM PLA2, 300 mM NaCl, and 50 mM $CaCl_2$ at pH 4.0 and 37 °C. The FID from 200 scans was processed with Gaussian multiplication (line broadening of −5, Gaussian broadening of 0.1) prior to Fourier transformation.

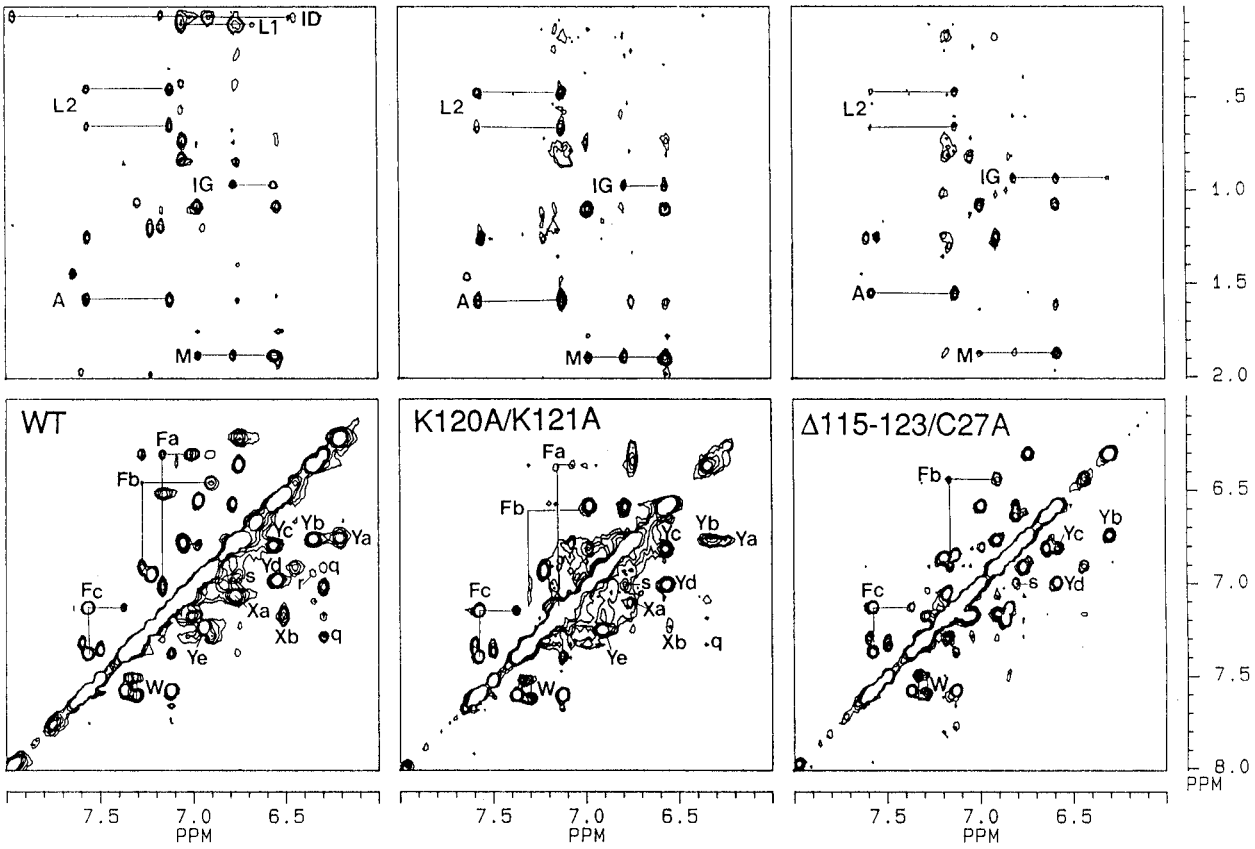

FIGURE 3: Phase-sensitive NOESY spectra of WT and the three mutants in D_2O at 500 MHz. The WT spectrum was reproduced from Dupureur et al. (1992a). Sample conditions were the same as in Figure 2. The mixing time was 200 ms. A 4096 × 512 matrix in the time domain was recorded and zero-filled to a 4096 × 2048 matrix prior to multiplication by a Gaussian function (line broadening of −3, Gaussian broadening of 0.1). The identified spin systems are labeled as followings: three of the four phenylalanines (Fa−Fc), five of the seven tyrosines (Ya−Ye), and the single tryptophan (W). Two of the unidentified spin systems are labeled as Xa and Xb. The NOE cross peaks p−s arise from Ya/Xa, Fa/Fb, Yb/Ye, and Yc/Yd, respectively.

reason for the missing resonances is that they are shifted significantly. If this is the case, it is noticeable that most of these residues are located at the active site (Y69 and F22), the hydrophobic channel (F5 and I9), or the calcium binding loop (Y28). The results suggest that the conformation of the deletion mutant is either little perturbed or perturbed only

Table 1: Chemical Shifts of the Assigned Residues for WT and Mutants[a]

spin system[b]	possible assignments[c]	WT			K120A/K121A			Δ115−123/C27A		
Fa	(F5)	6.28	7.00	7.15	6.35	7.07	7.16			
Fb	F106	6.43	6.88	7.26	6.59	6.99	7.30	6.44	6.91	7.17
Fc	F94	7.10	7.35	7.55	7.10	7.37	7.58	7.12	7.37	7.58
Ya	Y111	6.18	6.72		6.25	6.75				
Yb	Y52	6.34	6.74		6.32	6.75		6.32	6.74	
Yc	Y73	6.55	6.78		6.60	6.78		6.65	6.81	
Yd	Y75	6.52	6.95		6.58	6.98		6.59	7.00	
Ye	Y69	6.92	7.20		6.92	7.24				
W	W3	7.30	7.34	7.48	7.30	7.34	7.48	7.29	7.34	7.50
		7.58			7.58			7.58		
Xa	(F22)	6.75	7.04		6.78	7.08				
Xb	(Y28)	6.49	7.15		6.55	7.20				
ID	(I9)	0.05								
L1	(L41)	0.07								
L2	L58	0.44	0.63		0.44	0.63		0.48	0.64	
IG	I95	0.94			0.94			0.94		
A	(A55)	1.56			1.56			1.54		
M	(M8)	1.86			1.86			1.87		

[a] The underlined are resonances that differ by > 0.10 ppm between WT and mutant. [b] The designation of spin systems is based on previous work in this lab and other labs (Dupureur et al., 1992a,b; Fisher et al., 1989). [c] Parentheses indicate tentative assignments.

Table 2: Free Energy of GdnHCl-Induced Denaturation[a]

enzymes	$\Delta G_d^{H_2O}$ (kcal/mol)	$D_{1/2}$ (M)	m (kcal mol^{-1} M^{-1})
WT	9.5	6.9	1.5
K120A/K121A	12 (+2.5)	7.4	1.3
Δ115−123/C27A	5.7 (−3.8)	5.9	1.3

[a] Numbers in parentheses are differences in the values between mutants and WT, i.e., $\Delta\Delta G_d^{H_2O}$. The error limit in $\Delta G_d^{H_2O}$ is estimated to be ±0.5 kcal/mol.

Table 3: Summary of Kinetic Data for WT and Mutants[a]

	DC_8PC (0.1 M NaCl)		DC_8PC (4 M NaCl)		DC_8PM[b]	
enzyme	$K_{m,app}$ (mM)	$k_{cat,app}$ (s^{-1})	$K_{m,app}$ (mM)	$k_{cat,app}$ (s^{-1})	$K_{m,app}$ (mM)	$k_{cat,app}$ (s^{-1})
WT	0.72	650	0.09	1930	0.1	950
K120A/K121A	0.65	500	0.2	3200	0.1	840
Δ115−123/C27A	2.8	6	0.6	1000	0.06	300

[a] Obtained at 24 °C and pH 8.0. The estimated errors are ±15% on the basis of standard deviations of the fit. [b] The data for DC_8PM were the same within experimental errors in 0.1 and 4 M NaCl.

locally. The lack of major global conformational change is unexpected since deletion of nine C-terminal residues should have a greater impact on the conformation of the enzyme. Whether the possible local changes are related to the changes in the catalytic functions as described in this work remains to be established.

Conformational Stability. The conformational stability of all mutants was measured by GdnHCl-induced denaturation, monitored by CD spectroscopy. The data in Table 2 show that the conformational stability is appreciably perturbed for the deletion mutant; $\Delta G_d^{H_2O}$ is reduced by 3.8 kcal/mol for this mutant. On the other hand, the conformational stability of the mutant K120A/K121A is actually enhanced by 2.5 kcal/mol.

X-ray Crystallographic Analysis of K120A/K121A. As in our previous studies, we have used X-ray crystallography in addition to NMR to examine the possible changes in the global conformation of some of the mutants. In the present work, the double mutant K120A/K121A has been crystallized and its structure solved to a resolution of 1.9 Å. The stereoview of the electron density near the mutated residues 120 and 121 is shown in Figure 4a, and that of the catalytic triad residues Asp-99, His-48, and a water molecule is shown in Figure 4b. The overall RMS deviations from ideal values of bond lengths and bond angles are 0.014 Å and 2.87°, respectively. These geometric parameters suggest that the final atomic model has good overall stereochemistry. PROCHECK (Laskowski et al., 1993) was used to assess the quality of the protein model. All residues have (ϕ, ψ) angles in the allowed regions of the Ramachandran plot. The essential calcium is heptacoordinated, with $Ca^{2+}\cdots O$ distances ranging from 1.71 to 2.95 Å with an average distance of 2.31 Å. The RMS deviation between the C_α atoms of the mutant and the native enzyme is 0.39 Å, while that for the active site residues even smaller. The results indicate that the conformation of the backbone and the active site region of the mutant is remarkably similar to that of the WT, as shown in Figure 5.

Change of Substrate Specificity toward Micelles. As in the case of most of our studies with other mutants, the apparent kinetic constants $k_{cat,app}$ and $K_{m,app}$ of all mutants were determined for zwitterionic DC_8PC micelles and anionic DC_8PM micelles. The results listed in Table 3 show that the two mutants display significantly different properties. The double mutant K120A/K121A behaves essentially like WT, suggesting that the two lysine residues are not important for the catalytic function of PLA2 on zwitterionic or anionic micelles. On the other hand, the deletion mutant Δ115−123/C27A shows a significant change in the substrate specificity. Under the normal assay condition with 0.1 M NaCl present, the $k_{cat,app}$ of the deletion mutant decreases by a factor of 110 relative to that of WT for DC_8PC micelles, whereas it decreases by only a factor of 3 for DC_8PM micelles.

Restoration of Activity toward DC_8PC Micelles by NaCl. A possible explanation for the change of substrate specificity of the deletion mutant is that electrostatic interactions between the deletion mutant and the negatively charged micelles restore the mutant to the active conformation. To test this interpretation, we measured the activity of the mutant toward DC_8PC micelles in the presence of 4 M NaCl. As shown in Table 3, the $k_{cat,app}$ of the deletion mutant is restored from 6 to 1000 s^{-1}.

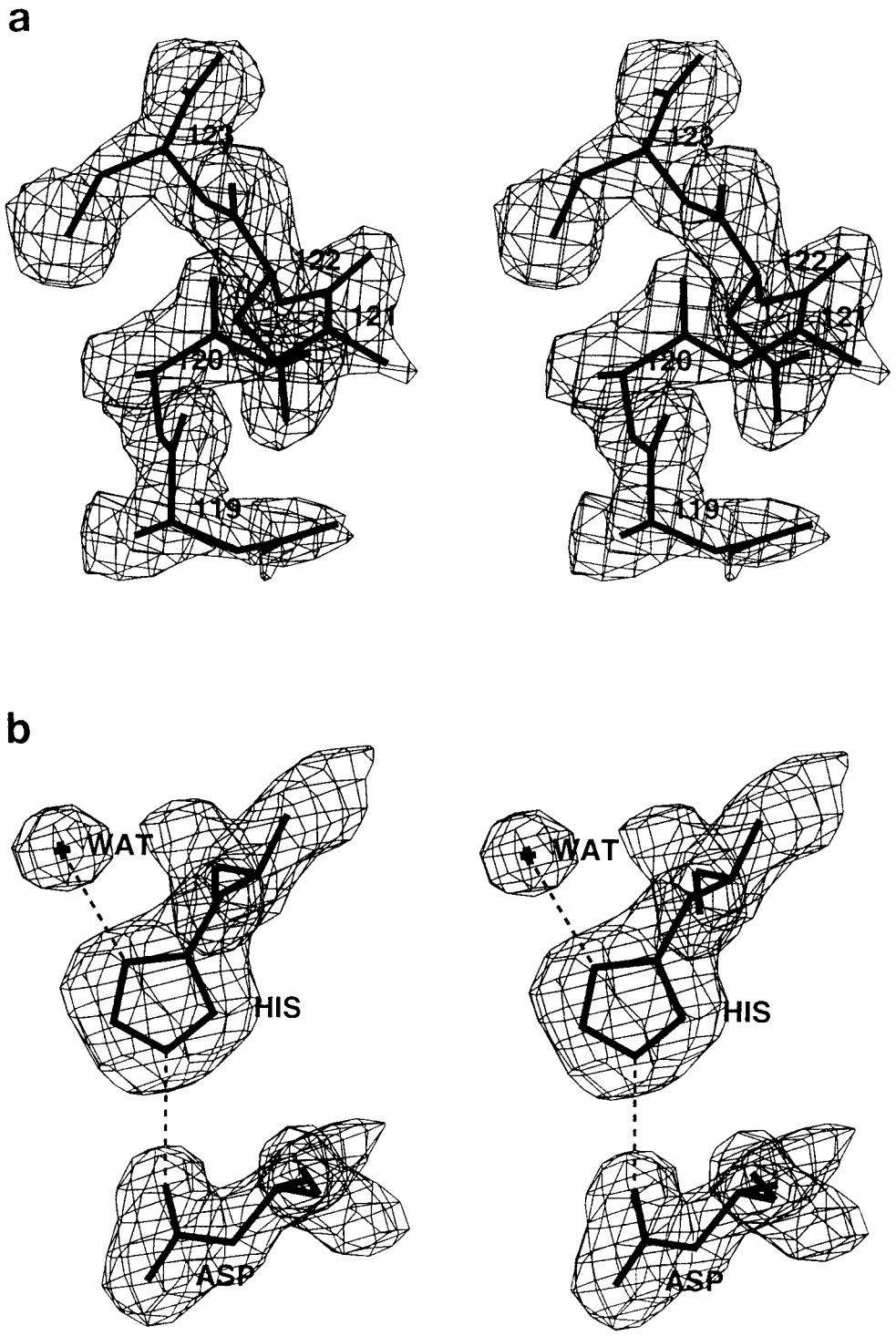

FIGURE 4: (a) Stereoview of the electron density around the mutated region in the ($2F_o - F_c$) omit map. The alanine methyl groups of residues 120 and 121 can be seen. (b) Stereoview of the electron density of the catalytic diad and the catalytic water in the ($2F_o - F_c$) omit map.

Rationales for Further Kinetic Analyses. The kinetic constants for micelle substrates do not differentiate the binding of the enzyme to the interface and the catalysis at the interface. In our past studies of WT PLA2 and its mutants, the kinetic behavior of the enzymes was further analyzed in detail in the scooting mode by use of anionic $DC_{14}PM$ vesicles. It is important to note that some of the binding constants were obtained from protection studies in the presence of neutral diluent deoxy-LPC, which is zwitterionic. In the past studies, these data were used together to describe the interfacial kinetic behavior since there were no significant differences between the activities of zwitterionic and anionic substrates. This is not the case for the deletion mutant Δ115−123/C27A as described in the previous two sections.

The following sections describe the experiments designed for understanding the nature of the change in the substrate specificity of the deletion mutant. At first, the E to E* binding step was examined by spectroscopic methods for both anionic and zwitterionic interfaces. This was followed by analyses of the E* to E*L (L being an active site-directed ligand) binding step for both anionic and zwitterionic interfaces. The chemical step for catalysis at the interface, E*S to E*P, was analyzed only for the anionic interface on $DC_{14}PM$ vesicles, since no such methods have been developed for zwitterionic vesicles.

FIGURE 5: Stereoview of the superposition of the α-carbon atoms of the double mutant K120A/K121A (solid line) and the wild type (dashed line). The RMS deviation is 0.39 Å between the double mutant and the wild type PLA2.

Binding Affinity of the Deletion Mutant to the Zwitterionic Interface Deoxy-LPC Is Not Significantly Perturbed. The equilibrium dissociation constant K_d at the zwitterionic interface was obtained by monitoring the fluorescence changes upon the binding of E to the interface of zwitterionic neutral diluent deoxy-LPC (Jain et al., 1993). Since the presence of 4 M NaCl restored the activity of the deletion mutant toward DC_8PC micelles, the dissociation constants were obtained in the absence and the presence of 4 M NaCl. The K_d values thus obtained are 7 mM (no salt) and 0.31 mM (4 M NaCl) for WT and 5 mM (no salt) and 0.56 mM (4 M NaCl) for the deletion mutant. The results suggest that the deletion mutant behaves in a manner similar to that of WT in binding to the zwitterionic interface in the absence and presence of 4 M NaCl. It is also pertinent to note that the binding constant (K_d^I) for the E−MJ33 complex in the aqueous phase to deoxy-LPC micelles is comparable for the deletion mutant and WT (ca. 0.25 mM in both cases).

Binding Affinity of the Deletion Mutant to the Anionic DTPM Vesicles Is Not Significantly Perturbed. Binding of PLA2 to the anionic DTPM vesicles was investigated by the change in fluorescence emission due to perturbation of the environment of Trp-3 (Jain & Maliwal, 1993; Jain et al., 1993). As shown in Figure 6, both WT and the deletion mutant titrated with the anionic DTPM vesicles show an increase in fluorescence emission at 333 nm. The sharp increase at low lipid concentrations indicates that the binding is of high affinity. The curves also suggest that the stoichiometry is the same but that the relative magnitudes are somewhat different between WT and the deletion mutant, possibly reflecting small changes in the local environment of Trp-3.

The results of the spectroscopic studies in this and the previous sections indicate that the deletion mutant behaves in a manner similar to that of WT in the binding affinity of the E to E* step for both anionic and zwitterionic interfaces. The results do not offer an explanation for the different specificity between WT and the deletion mutant toward anionic and zwitterionic substrates. We therefore compared the E* to E*L step between zwitterionic and anionic interfaces, as described in the following two sections.

E to E*L at the Zwitterionic Interface Is Significantly Perturbed.* The equilibrium dissociation constants at the

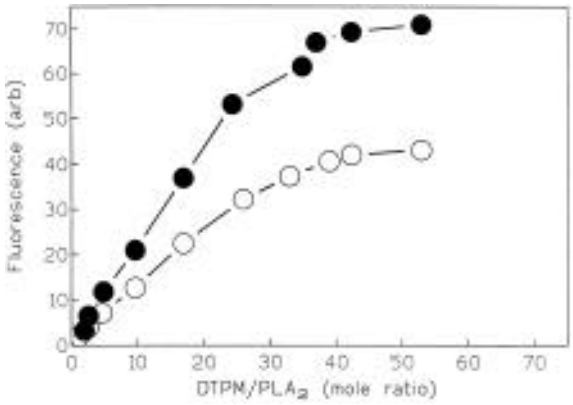

FIGURE 6: Relative change in the fluorescence emission intensity at 333 nm on the addition of DTPM vesicles to 2 μM WT (open circles) and the deletion mutant (closed circles) in 0.1 mM $CaCl_2$ and 10 mM Tris at pH 8.0. The ordinate is expressed as the lipid/enzyme mole ratio on the outer monolayer of vesicles. As expected, essentially similar behavior was observed in the absence of calcium because calcium is not required for the binding of the enzyme to the interface.

zwitterionic interface for inhibitors (K_I*), the products of hydrolysis (K_P*), calcium (K_{Ca}*), and substrate analog DTPM (K_S*) were determined by monitoring the rate of alkylation of His-48 in the presence of the neutral diluent deoxy-LPC and the appropriate ligand as described previously (Jain et al., 1991a). The results in Table 4 show that the double mutant K120A/K121A again behaves in a manner similar to that of WT, but the deletion mutant Δ115−123/C27A displays significantly higher dissociation constants for active site-directed ligands at the zwitterionic interface.

Equilibrium and Catalytic Constants at the Anionic Interface. The binding and kinetic parameters at the *anionic* interface were obtained by performing detailed analyses using $DC_{14}PM$ vesicles. The protocols for monitoring interfacial catalysis in the scooting mode have been described in Jain et al. (1986, 1991c, 1995) and Berg et al. (1991). The intrinsic rate of the catalytic turnover can be best seen in the values of v_o, the steady state rate of hydrolysis of DC_{14}-PM vesicles at the mole fraction of substrate $X_S = 1$. The results are summarized in Table 5. The reaction progress curves for the hydrolysis of $DC_{14}PM$ by the double mutant and the deletion mutant in the form of small sonicated

Table 4: Equilibrium Dissociation Constants of E*L at Zwitterionic Interface[a]

parameters	WT	K120A/ K121A	Δ115−123/ C27A
alkylation time[b]			
E (min)	<1	2	35
E* (min)	1.5	3	25
K_{ND}*	>1	>1	1
K_I* (MJ33)	0.01	0.004	0.35
K_S* (DTPM)	0.02	0.01	0.21
K_P* (product of $DC_{14}PM$)	0.025	0.01	0.12
K_{Ca} (mM)	0.5	1.6	>3
K_{Ca}* (mM)	0.35	0.49	1

[a] The error limits are estimated to be ±15% for the values in this table. [b] The alkylating agent used is p-nitrophenacyl bromide for WT and K120A/K121A and phenacyl bromide for Δ115−123/C27A.

Table 5: Catalytic and Equilibrium Parameters for the Hydrolysis of $DC_{14}PM$ by WT and Mutants[a]

parameters	WT	K120A/ K121A	Δ115−123/ C27A
v_o (s^{-1})	330	90	25
$X_I(50)$ MJ33	0.025	0.01	0.02
K_{Ca}*(S) (mM)	0.15	0.16	0.5
v_o/N_SKi	11	45	8.3
K_M* from			
K_{P*} and RPC	0.4	0.45	0.9
$X_I(50)$	0.65	0.66	−
K_{Ca}*(S)	0.7	0.48	0.7
k_{cat} (s^{-1})	500	140	50

[a] The error limits are estimated to be ±15% for the values in this table.

vesicles were apparently first-order (data not shown). These results were obtained under conditions where there is an excess of vesicles and the enzyme-containing vesicles have at most one enzyme molecule per vesicle. The ratio v_o/N_Sk_i for the two mutants are also compared in Table 5. In addition, analysis of the whole reaction progress curves indicated that the affinity of the enzyme to the anionic vesicle interface (i.e., the E to E* step) has not been perturbed to a noticeable extent. In both the double mutant and the deletion mutant, the initial phase of activity ceased before all the substrate present in the reaction mixture was hydrolyzed, and the extent of hydrolysis per enzyme molecule was the same as with WT. Since the reaction essentially stopped at the end of this phase, it suggested that the intervesicle exchange of enzyme molecules is essentially negligible over the time course of the reaction.

Values of k_{cat} were obtained from the relationship $k_{cat} = v_o(1 + K_M^*)$. Values of K_M* were calculated from initial rates of hydrolysis of $DC_{14}PM$ in the absence and presence of the competitive inhibitor MJ33 [$(v_o)^\circ$ and $(v_o)^I$, respectively] according to the following equation (Jain et al., 1991a):

$$(v_o)^\circ/(v_o)^I = 1 + [(1 + 1/K_I^*)/(1 + 1/K_M^*)][X_I/(1 - X_I)] \quad (1)$$

where X_I is the mole fraction of the inhibitor and K_I* is the dissociation constant of the inhibitor. In addition, K_M* was also calculated from its relationship with K_{Ca}*(S) and K_{Ca}* values (Yu et al., 1993):

$$K_{Ca}^*(S) = K_{Ca}^*/(1 + 1/K_M^*) \quad (2)$$

where the apparent dissociation constant of PLA2 for calcium under kinetic conditions, K_{Ca}*(S), was obtained from the dependence of v_o on the calcium concentration. As the third approach, K_M* was calculated from the relationship of K_P* and the rate parameters obtained from the integrated reaction progress curve (Berg et al., 1991), where $N_Sk_i/v_o = (1 + 1/K_M^*)/(1 + 1/K_P^*)$.

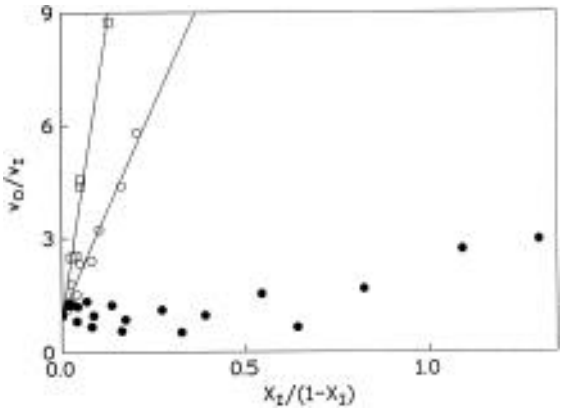

FIGURE 7: Plots of v_o/v_I versus $X_I/(1 - X_I)$ for MJ33 and the deletion mutant in the presence of 0.1 M NaCl and DC_8PC (filled circles), 4 M NaCl and DC_8PC (open circles), and 0.001 M NaCl and $DC_{14}PM$ (squares). Experiments were performed in 4 mL of water containing the appropriate concentrations of NaCl and 10 mM $CaCl_2$ (for DC_8PC) or 1 mM $CaCl_2$ (for $DC_{14}PM$), at pH 8.0 and 25 °C. Data points were derived from several trials, all of which contain substrates at concentrations well above its critical micelle concentration.

The data in Table 5 indicate modest (a factor of ca. 10) decreases in v_o and k_{cat} for the deletion mutant at the anionic interface. The values of K_M* for $DC_{14}PM$ were about 0.65 mole fraction for WT and the double mutant. As noted earlier, the corresponding interfacial catalytic constants cannot yet be obtained at the zwitterionic interface. As described in the following sections, a surprising anomaly was seen with the deletion mutant. On the anionic interface, it binds active site-directed ligands (E* to E*L or E* to E*I) with affinity comparable to that seen with the double mutant or WT. However, at the zwitterionic interfaces, the binding of the ligands to the deletion mutant is of low affinity and does not show an obligatory requirement for calcium.

The E to E*L Step of the Deletion Mutant Depends on the Interface*. The $X_I(50)$ value of MJ33, an active site-directed ligand, does not change between WT and the mutants (Table 5); however, the K_I* value of MJ33 increases from 0.01 for WT to 0.35 for the deletion mutant (Table 4). Both parameters measure the binding affinity of MJ33; the $X_I(50)$ value was determined on the basis of the inhibition of the hydrolysis of *anionic* $DC_{14}PM$ vesicles by MJ33, while the K_I* value was determined with *zwitterionic* micelles on the basis of the ability of MJ33 to protect from alkylation. The K_S* and K_P* values in Table 4 are also higher for the deletion mutant relative to those of WT.

A particularly striking result showing the effects of interface and high salt concentrations on $X_I(50)$ for MJ33 is shown in Figure 7, where the relative rate of hydrolysis v_o/v_I of the deletion mutant is plotted against $X_I/(1 - X_I)$ in accordance with the relationship in eq 1. As shown in this figure, hydrolysis of anionic substrate $DC_{14}PM$ (squares) shows an expected dependence on the mole fraction of MJ33, while hydrolysis of zwitterionic substrate DC_8PC at low salt concentrations (full circles) shows little dependence on the mole fraction of MJ33. However, the effect of MJ33 on the hydrolysis of DC_8PC is restored upon addition of 4 M

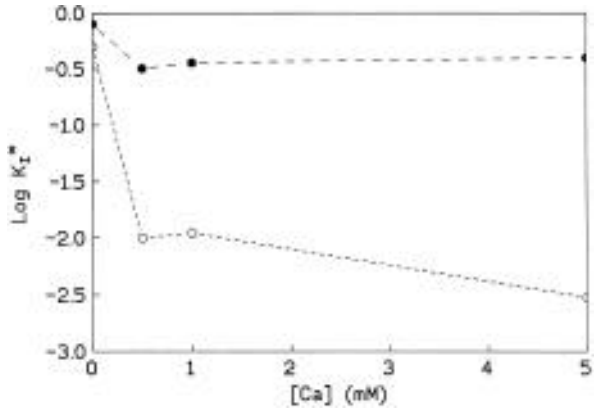

FIGURE 8: Dependence of K_I* for MJ33 bound to WT (open circles) or the deletion mutant (filled circles) on the calcium concentration. The incubation was carried out at 0.1 M NaCl and 50 mM cacodylate buffer in the presence of 1.65 mM deoxy-LPC.

NaCl (open circles). It may be remarked here that partitioning of chloride anion in the zwitterionic micelles imparts a net anionic character (M. K. Jain et al., in preparation). These results taken together suggest that the E* to E*I step is impaired in the deletion mutant at the zwitterionic but not at the anionic interface. This can partially account for the preference of the deletion mutant for the hydrolysis of anionic micelles relative to zwitterionic micelles.

Calcium Binding and Ligand Binding are Uncoupled in the Deletion Mutant. The data in Tables 4 and 5 indicate that the calcium dissociation constants K_{Ca} and K_{Ca}* and K_{Ca}*(S) of the deletion mutant increase relative to those for the WT, though by only factors of 3−6. Such a change in calcium binding affinity, though small, led us to examine whether the low affinity of MJ33 to the active site at the zwitterionic interface is related to the perturbed role of calcium as the cofactor. The result suggests an "uncoupling" between calcium binding and MJ33 binding for the deletion mutant. It has been well-established that calcium is an obligatory cofactor for binding of active site-directed ligands to WT PLA2 (Yu et al., 1993), and the K_I* values listed in Table 4 were obtained in the presence of Ca^{2+}. As shown in Figure 8, addition of calcium ions causes the K_I* of MJ33 to decrease (higher affinity) by a factor of ca. 60 for WT PLA2 in the presence of 0.1 M NaCl but has little effect on the K_I* of the deletion mutant.

The results from this and the previous section taken together suggest that, at low salt concentrations on zwitterionic interfaces, the affinity of the deletion mutant for active site-directed ligands is poor because the obligatory coupling between the calcium and substrate binding is lost.

DISCUSSION

The results of this work indicate that the double mutant K120A/K121A behaves in a manner similar to that of WT PLA2 in all of the properties we have examined, whereas the deletion mutant Δ115−123/C27A displays a significant change in the substrate−cofactor coupling reflected as a change in the specificity toward zwitterionic and anionic micelles. Detailed spectroscopic and kinetic analyses suggest that the change in the substrate specificity of the deletion mutant was not caused by a change in the E to E* step. It was caused partially by a change in the E* to E*L step at the zwitterionic interface, which could in turn be related to the inability of Ca^{2+} to enhance the binding of substrate or inhibitor. It is also implicit in these results that the anionic interface is somehow able to regulate the coupling between the binding of calcium and the substrate. The implications of these findings in the structure−function relationship of PLA2 are further elaborated in the following sections.

Lys-120 and Lys-121 Are Unimportant for Structure or Function. These two positively charged residues appear to be unimportant for the structure or function of PLA2. The K120A/K121A double mutant behaves in a manner very similar to that of WT PLA2 in the conformational analysis by NMR, conformational stability, fluorescence analysis of the E to E* step, binding of ligands to the active site, and kinetic assays under various conditions. Like the C27A/C123A disulfide mutant (Zhu et al., 1995), the conformational stability of this mutant increases by 2.5 kcal/mol relative to that of WT, as shown in Table 2.

Earlier attempts to ascertain the role of the lysine residues at the C-terminus deserve a comment. Acylation of lysines has been shown to alter the binding of the enzyme to zwitterionic interface without any effect on the catalytic properties (Van der Wiele et al., 1988). This is consistent with our results, except that in their study partitioning of the acyl chains probably led to enhanced binding of the enzyme to the interface. On the other hand, Dua et al. (1995) asserted that the lysines at the N-terminus are "essential" for the function of bovine pancreatic PLA2. Our results do not support this assertion.

The C27-C123 Disulfide Bond Plays Only a Marginal Role. The C27−C123 disulfide bond is absolutely conserved among the 46 natural variants of PLA2 whose sequences have been aligned by Heinrikson (1991). On the basis of the crystal structure of PLA2, this disulfide bond serves to "fix" the C-terminus segment and possibly also the calcium binding loop (the residues 28−32 segment). Thus, one would expect that deletion of this disulfide bond might have a deleterious effect on the structure of PLA2. This is not the case when this disulfide bond and the C-terminal segment are deleted altogether, as described in this work. In a separate report (Zhu et al., 1995), each of the seven disulfide bonds of PLA2 has been deleted separately. Consistent with the results reported here, the kinetic constants of C27A/C123A are within a factor of 5 of those of WT, the proton NMR property is little perturbed, and the free energy of denaturation actually *increases* by 2.4 kcal/mol. Thus, this absolutely conserved disulfide bond appears to have a marginal effect on either the structure or the catalysis of PLA2.

Possible Roles of the C-Terminal Segment in Interfacial Binding and Catalysis. It is surprising that deletion of nine C-terminus residues caused only localized rather than global changes in the conformation of PLA2. The lack of major conformational change ensures that the functional data of the deletion mutant can be interpreted quantitatively. Most of the residues on the C-terminal segment are located at the edge of the i-face, which has been suggested to be involved in the interfacial binding (Ramirez & Jain, 1991). These C-terminus residues are very highly conserved among the pancreatic enzymes, though not among the broader sources of PLA2 (Heinrikson, 1991). Thus, one would expect to see large functional effects when the entire segment is deleted. However, the only functional change observed was a significant decrease in the $k_{cat,app}$ of zwitterionic substrates, and the decrease in $k_{cat,app}$ can be restored by addition of a high salt concentration.

Fluorescence spectroscopic studies indicated that the differentiation does not lie in the binding affinity of the E to E* step at the zwitterionic or anionic interface. Further determination of equilibrium dissociation constants suggested that the ligand binding to the active site (E* to E*L) is perturbed at the zwitterionic interface but not at the anionic interface. The effect appears to be related to the cofactor role of calcium ions. Calcium is known to stimulate binding of substrates or inhibitors to the active site of PLA2 (Yu et al., 1993). However, such an effect is lacking or very small for the deletion mutant (Figure 8).

The fact that deletion of the C-terminus fragment does not cause a significant change in the binding affinity of the E to E* step for either zwitterionic or anionic interface should *not* be used to conclude that the C-terminus segment is not involved in the interfacial binding of PLA2. Other data suggest that the C-terminus segment should be involved in the interfacial binding since the deletion mutant can only function properly at an anionic interface. On the zwitterionic interface, Ca^{2+} is unable to facilitate the binding of inhibitor or substrate to the active site and the catalytic activity is significantly reduced.

As we have concluded previously from the study of N-terminal residues (Liu et al., 1995; Maliwal et al., 1994), the interfacial site involves a large number of residues (Dijkstra et al., 1981; Ramirez & Jain, 1991) and the effects of modifying individual residues are small. Even the effects of deleting the entire C-terminal segment are modest at best. The same is true for N-terminal residues (Liu et al., 1995; Maliwal et al., 1994), Leu-31 (Kuipers et al., 1990), and Lys-56 (Noel et al., 1990, 1991). This phenomenon is consistent with the fact that the enzyme can accept interfaces with a broad range of phospholipids with different head groups and in different physical states. It also supports the notion that PLA2 exists in an ensemble of conformations which can adapt to a range of interfaces (Jain & Maliwal, 1993; Maliwal et al., 1994). Thus, although the tertiary structure of PLA2 is rigidly defined by seven disulfide bonds, it can adapt for different constraints of interfacial binding.

REFERENCES

Berg, O. G., Yu, B.-Z., Rogers, J., & Jain, M. K. (1991) *Biochemistry 30*, 7283−7297.

Brunger, A. T. (1992) *X-PLOR Manual*, Yale University, New Haven, CT.

Cajal, Y., Rogers, J., Berg, O. G., & Jain, M. K. (1996) *Biochemistry 35*, 299−308.

Deng, T., Noel, J. P., & Tsai, M.-D. (1990) *Gene 93*, 229−234.

Dijkstra, B. W., Drenth, J., & Kalk, K. H. (1981) *Nature 289*, 604−606.

Dijkstra, B. W., Kalk, K. H., Drenth, J., de Haas, G. H., Egmond, M. R., & Slotboom, A. J. (1984) *Biochemistry 23*, 2759−2766.

Dua, R., Wu, S., & Cho, W. (1995) *J. Biol. Chem. 270*, 263−268.

Dupureur, C. M., Yu, B.-Z., Jain, M. K., Noel, J. P., Deng, T., Li, Y., Byeon, I.-J. L., & Tsai, M.-D. (1992a) *Biochemistry 31*, 6402−6413.

Dupureur, C. M., Yu, B.-Z., Mamone, J. A., Jain, M. K., & Tsai, M.-D. (1992b) *Biochemistry 31*, 10576−10583.

Fisher, J., Primrose, W. U., Roberts, G. C. K., Dekker, N., Boelens, R., Kaptein, R., & Slotboom, A. J. (1989) *Biochemistry 28*, 5939−5946.

Heinrikson, R. L. (1991) *Methods Enzymol. 197*, 201−214.

Jain, M. K., & Gelb, M. H. (1991) *Methods Enzymol. 197*, 112−125.

Jain, M. K., & Maliwal, B. P. (1993) *Biochemistry 32*, 11838−11846.

Jain, M. K., Rogers, J., Jahagirdar, D. V., Marecek, J. F., & Ramirez, F. (1986) *Biochim. Biophys. Acta 860*, 435−447.

Jain, M. K., Yu, B.-Z., Rogers, J., Ranadive, G. N., & Berg, O. G. (1991a) *Biochemistry 30*, 7306−7317.

Jain, M. K., Rogers, J., Berg, O. G., & Gelb, M. H. (1991b) *Biochemistry 30*, 7340−7348.

Jain, M. K., Tao, W., Rogers, J., Arenson, C., Eibl, H., & Yu, B.-Z. (1991c) *Biochemistry 30*, 10256−10268.

Jain, M. K., Yu, B.-Z., Rogers, J., Gelb, M., Tsai, M.-D., Hendrickson, E., & Hendrickson, S. (1992) *Biochemistry 31*, 7841−7847.

Jain, M. K., Yu, B.-Z., & Berg, O. G. (1993) *Biochemistry 32*, 11319−11329.

Jain, M. K., Gelb, M. H., Rogers, J., & Berg, O. G. (1995) *Methods Enzymol. 249*, 567−614.

Jones, T. A. (1985) *Methods Enzymol. 115*, 157−171.

Kuipers, O. P., Kerver, J., Van Meersbergen, J., Vis, R., Dijkman, R. M., Verheij, H. M., & de Haas, G. H. (1990) *Protein Eng. 3*, 599−603.

Laskowski, R. A., Mac Arthur, M. W., Moss, D. S., & Thornton, J. M. (1993) *J. Appl. Crystallogr. 26*, 283−291.

Li, Y., & Tsai, M.-D. (1993) *J. Am. Chem. Soc. 115*, 8523−8526.

Liu, X., Zhu, H., Huang, B., Rogers, J., Yu, B.-Z., Kumar, A., Jain, M. K., Sundaralingam, M., & Tsai, M.-D. (1995) *Biochemistry 34*, 7322−7334.

Maliwal, B. P., Yu, B.-Z., Szmacinksi, H., Squier, T., Binsbergen, J. V., Slotboom, A. J., & Jain, M. K. (1994) *Biochemistry 33*, 4509−4516.

Noel, J. P., Deng, T., Hamilton, K. J., & Tsai, M.-D. (1990) *J. Am. Chem. Soc. 112*, 3704−3706.

Noel, J. P., Bingman, C., Deng, T., Dupureur, C. M., Hamilton, K. J., Jiang, R.-T., Kwak, J.-G., Sekharudu, C., Sundaralingam, M., & Tsai, M.-D. (1991) *Biochemistry 30*, 11801−11811.

Nozaki, Y. (1972) *Methods Enzymol. 26*, 43−50.

Pace, C. N. (1986) *Methods Enzymol. 131*, 266−280.

Ramirez, F., & Jain, M. K. (1991) *Proteins 9*, 229−239.

Sanger, F., Niklen, S., & Coulson, A. R. (1977) *Proc. Natl. Acad. Sci. U.S.A. 74*, 5463−5467.

Scott, D. L., White, S. P., Otwinowski, Z., Yuan, W., Gelb, M. H., & Sigler, P. B. (1990) *Science 250*, 1541−1546.

Van den Berg, B., Tessari, M., de Haas, G. H., Verheij, H. M., Boelens, R., & Kaptein, R. (1995) *EMBO J. 14*, 4123−4131.

Van der Wiele, F. C., Atsma, W., Dijkman, R., Schreus, A. M. M., Slotboom, A. J., & de Haas, G. H. (1988) *Biochemistry 27*, 1683−1688.

Yu, B.-Z., Berg, D. G., & Jain, M. K. (1993) *Biochemistry 32*, 6485−6492.

Zhu, H., Dupureur, C. M., Zhang, X., & Tsai, M.-D. (1995) *Biochemistry 34*, 15307−15314.

BI960234O